DOI: 10.2478/auoc-2025-0018

Ovidius University Annals of Chemistry Volume 36, Issue 2, pp. 149 - 161, 2025

Synthesis and *in-silico* analysis of some 4-bromophenyl enones

Pandiyan SUDHA,[1] Subramanian BALASUNDARI,[1] Paneerselvam GAYATHRI,[1] Shanmugasundaram RAJASRI,[2] Inbasekaran MUTHUVEL,[1,3] Palanippan SIVAKUMAR,[4] Venkatesan MANIKANDAN,[5] Subramanian SRINIVASAN,[6] Vasudevan SATHIYENDIRAN,[7] and Ganesamoorthy THIRUNARAYANAN[*,1]

[1]*Department of Chemistry, Annamalai University, Annamalainagar-608002, India*
[3]*Department of Chemistry, Raak College of Engineering and Technology, G. N. Palayam, Villiyanur, Puducherry-605110, India*
[3]*Department of Chemistry, M. R. Government Arts College, Mannargudi-614001, India*
[4]*Department of Chemistry, Aringnar Anna Government Arts College, Villupuram-605602, India*
[5]*Department of Chemistry, Shree Ragavendra Arts and Science College, Keelamoongiladi-608602, Chidambaram, India*
[6] *Chemistry Wing, Centre for Distance & Online Education, Annamalai University, Annamalainagar-608002, India*
[7]*Department of Chemistry, Sourashtra College, Madurai-625004, India*

Abstract. Nine substituted styryl 4-bromophenyl ketones were synthesized by potassium hydrogen phthalate ($KHC_6H_4O_4$) assisted crossed-aldol condensation of 4-bromoacetophenone and benzaldehydes in stirring method. This method yields more than 80 % product. In this condensation, the effect of solvents was studied. The purities of these enones were analyzed by their data reported earlier in literature. The molecular structure of 4-bromophenyl chalcones was investigated using Density Functional Theory (DFT) at the B3LYP/6-311G(d,p) level of theory. The simulations provide insights into total energy, frontier molecular orbitals (HOMO and LUMO), and molecular electrostatic potential (MEP) surfaces. Molecular docking analysis of 4-bromophenyl chalcones against D-glutamate ligase (PDB ID:1UAG) bacterial protein that gives highest binding affinity value -6.63 with the compound **1c.** ADMET results support the further development of pharmacologically active drugs. The enzyme target prediction ligand-based method demonstrates 4-bromophenyl chalcone derivatives (**1a-i**) effective inhibitors of oxidoreductase, kinases, and proteases enzymes. These findings revealed 4-bromophenyl chalcone derivatives as potential candidates for therapeutic applications.

***Keywords*:** potassium hydrogen phthalate; crossed-aldol condensation; 4-bromophenyl chalcone; DFT; molecular docking; ADMET studies.

1. Introduction

Chalcones are an essential component for the formation of pharmacologically active heterocyclic molecules. Chalcones have an α, β-unsaturated moiety; this moiety enhances the biological activity of the chalcones. Due to the presence of α, β-unsaturation and carbonyl group, chalcones have various biological activities like antibacterial [1, 2], antioxidant [2], antifungal [3], anticancer [4], antimalarial [5], antidiabetic [6], anti-inflammatory, analgesic [7], antiviral [8], and anti-tubercular [9] activities. Different kinds of methods are available for the synthesis of chalcones, like aldol condensation, crossed aldol condensation, Claisen-Schmidt condensation, and Knoevenagel reactions [10, 11]. To synthesize chalcones by the condensation method, various catalysts are available, like greener catalysts, acidic catalysts, and basic catalysts [12]. The world interacts with electronic devices and moves into the digital age in the twenty-first century. Computers are at the intersection of everything, and they are also very helpful in the fields of science and medicine. For the purpose of determining the pharmacokinetics and biological characteristics of the desired organic molecules, the ADMET (absorption, distribution, metabolism, excretion, and toxicity) properties prediction plays a vital role in understanding the biological properties of drug design [13]. The presence of halogens in the chalcone moiety enhances the therapeutic properties of chalcones [14].

In the present work, a series of 4-bromophenyl chalcone derivatives have been successfully synthesized and characterized. We used computational tools, like ADMET prediction analysis, to gain deeper insights into the molecular behavior and biological efficacy of the synthesized chalcone derivatives. We conducted pharmacokinetic evaluations, molecular docking studies with potential protein targets, and quantum chemical calculations using DFT at the B3LYP/6-311G(d,p) level. This study enhances the current knowledge of chalcones and their potential therapeutic uses,

* Corresponding author. *E-mail address:* thirunarayanan.g.10313@annamalaiuniversity.ac.in (Ganesamoorthy Thirunarayanan)

potentially contributing to the design of more effective and selective drug candidates.

2. Experimental

2.1. Reagents and methods

Chemicals and solvents employed for this study were procured from Sigma-Aldrich chemical company, Bengaluru, India and not purified further. The melting points of the enones, representing their physical constants, were determined using a Raga-Tech apparatus and open capillaries. FT-IR spectra (4000–400 cm^{-1}) of the synthesized compounds were recorded using a Bruker 300 FT-IR spectrophotometer with KBr pellets. NMR measurements were carried out on a Bruker AV-III 500 spectrometer operating at 400 MHz for ^{1}H and 100 MHz for ^{13}C, using deuterated chloroform ($CDCl_3$) as the solvent and tetramethylsilane (TMS) as the internal reference. Elemental (CHN) analysis of the ketones was performed with a Perkin Elmer 240C analyzer. The mass spectra of all synthesized 4-bromophenyl enones were obtained in electron ionization (EI) mode using a Shimadzu ICPMS-2030 class mass spectrometer.

2.2. Synthesis of 4-bromophenyl chalcone derivatives (1a - i)

In a 150 mL stoppered conical flask, an equal molar amounts of 4-bromo acetophenone (1 mmol) and substituted benzaldehydes (1 mmol), and 10 mL of ethanol were taken. To this mixture, 2 mL of 5 M potassium hydrogen phthalate was added and stirred for 25 min in a magnetic stirrer (Scheme 1). After 25 min, the resulting pale-yellow precipitate was collected using a filtration pump, rinsed with water, and dried. Recrystallization of the crude enone was carried out using ethanol, and purified compound was stored in a desiccator.

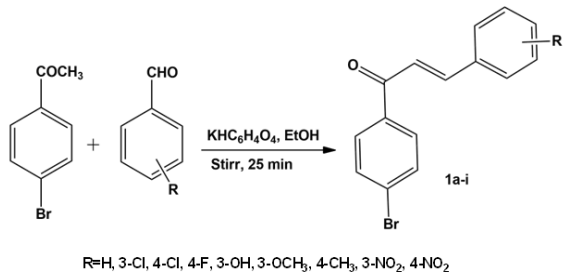

Scheme 1. Potassium hydrogen phthalate assisted synthesis of (2*E*)-substituted styryl-4-bromophenyl ketones (**1a-i**)

2.3. Density functional theory (DFT)

Gaussian 09 web tool was utilized for the density functional theory (DFT) analysis of the synthesized compounds, and Gauss View 6.0 software was used for visualization [15, 16]. The B3LYP/6-311G (d, p) basis set level was applied to optimize the lead compound's structural coordinates without any symmetry limitations [17, 18]. From the optimized geometry, the compound's energy and molecular electrostatic potential (MEP) profile were derived. Using Koopman's approximation, the HOMO–LUMO gap along with key chemical reactivity descriptors such as electronegativity, chemical potential, hardness, softness, and electrophilicity was determined.

2.4. Molecular docking analysis

Molecular docking studies were conducted using the 3D protein crystal structure downloaded from the Protein Data Bank (PDB) available at https://www.rcsb.org. The ligand's 2D and 3D structures are obtained by using ChemDraw 8.0. The docking studies are done by AutoDock tools software [3,13,18-20]. The selected protein is prepared by adding polar hydrogens, Kollman, and computer Gasteiger charges with removal of water molecules. The auto grid program was performed to create the grid maps of (120 x 70 x 60) A° grid points. The autodock results were finally analyzed with the help of Discovery Studio 2021 version. The results obtained from the molecular docking studies contribute to further research development of drug discovery.

2.5. ADMET study evaluation

In silico drug-likeness prediction evaluates whether a specific pharmacological agent exhibits characteristics that are suitable for being an orally active medication. The absorption, distribution, metabolism, excretion, and drug-likeliness of the synthesized compound can be determined by the SwissADME software [18, 20]. The Lipinski rule of five, a previously developed idea by Lipinski, serves as the foundation for this prediction. The SwissADME program was used to estimate pharmacokinetic parameters and other molecular features. The process was described after converting the synthesized compound's structure of **(1a-i)** to its canonical SMILE. This tool provides detailed information on physicochemical properties, including molecular weight, number of rotatable bonds (NROTB), hydrogen bond donors and acceptors, topological polar surface area (TPSA), Lipinski violations, and bioavailability score. The SwissADME also provides pharmacokinetic properties of the synthesized compound. To find the rate of absorption (%), the following equation (1) was used:

$$\%\, ABS = 109 - 0.345 \times TPSA \quad (1)$$

The toxicity effects of the synthesized compounds are obtained from Pro-toxicity software. These results are helpful to determine the biological efficiency of the compounds.

2.6. Secondary enzymatic target prediction

The Swiss Institute of Bioinformatics produced the "Swiss Target Prediction" bioinformatics software, which was utilized to determine the secondary enzymatic targets for the synthesized molecules [23]. To anticipate targets, this software uses the similarity concept approach, more especially reverse screening. In order to find comparable molecules against 3068 protein targets, a large library of experimentally known bioactive compounds 376, and 342 (2D and 3D), must be searched. From the top 15 predictions, the projected targets for this investigation were chosen, with the highest likelihood of interacting with the synthesized chemicals being given precedence. This data supports more research into the pharmacological effects of the

substances and enhances our understanding of their mode of action [17].

3. Results and discussion

3.1. Enone chemistry

In the experimental section, as we mentioned above, the substituted styryl 4-bromo enones were synthesized by the stirring method. Benzaldehydes having electron-donating substituents gave higher yields than electron-withdrawing substituents. The purity of the synthesized enones was confirmed through physicochemical, analytical, and spectroscopic data, all of which support the successful formation of the enones. The physical constants, yield and time required for the synthesis of (2*E*)-substituted styryl-4-bromophenyl ketones are tabulated in Table 1.

Table 1. Physical constants, time, yield and analytical data of (2*E*)-substituted styryl-4-bromophenyl ketones

Entry	X	M.F.	M.W.	Time (m)	Yield (%)	M.P. (°C)
1a	H	$C_{15}H_{11}BrO$	287	25	87	156-158 (157) [14]
1b	3-Cl	$C_{15}H_{10}BrOCl$	321	25	89	122-123 (120) [14]
1c	4-Cl	$C_{15}H_{10}BrOCl$	321	25	88	117-118 (115) [14]
1d	4-F	$C_{15}H_{10}BrOF$	305	25	85	142-143 (141) [14]
1e	3-OH	$C_{15}H_{11}BrO_2$	303	25	83	110-111
1f	3-OCH_3	$C_{16}H_{13}BrO_2$	321	25	90	195-196
1g	4-CH_3	$C_{16}H_{13}BrO$	305	25	89	150-151 (148) [14]
1h	3-NO_2	$C_{15}H_{10}BrO_3N$	332	25	80	126-127 (128) [14]
1i	4-NO_2	$C_{15}H_{10}BrO_3N$	332	25	82	135-136 (136) [14]

This condensation reaction followed acid-catalyzed reaction mechanism. First, the carbonyl oxygen of the ketone was protonated, followed by the formation of an enol. During the second step, nucleophilic attack by the enol on the carbonyl carbon of the aldehyde generates an alkoxide intermediate, with the carbonyl oxygen acquiring a negative charge and the enol carbon developing a partial positive charge. The third step is the loss of a proton from enol and the protonation of the negative charge of the oxygen atom of the aldehydic carbonyl group, which occur simultaneously. Finally, beta-elimination leads to afforded enones by the removal of water molecules. The proposed mechanistic pathway of this condensation was depicted in Scheme 2.

In this condensation, the influence of solvents on the yield was examined with various solvents such as ethanol, methanol, acetonitrile, dioxane, dichloromethane, isopropanol, and tetrahydrofuran. From the examination, the ethanol medium gave a higher yield than acetonitrile. The solvent influence on the yield of this condensation was presented in Table 2.

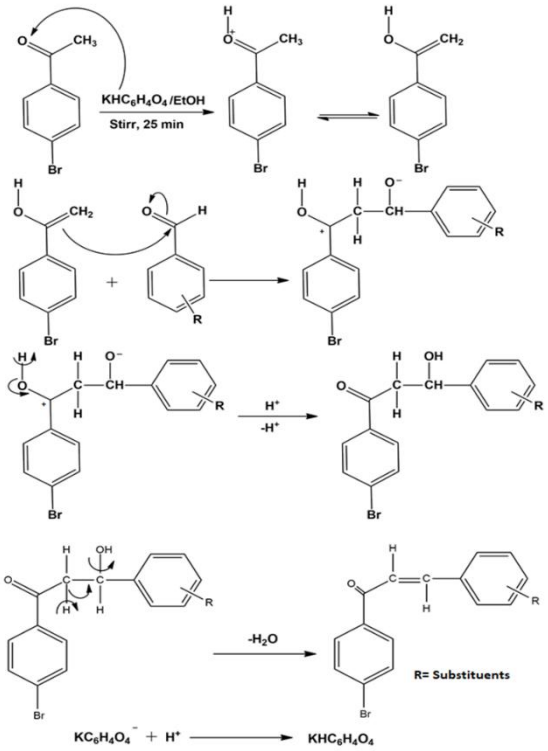

Scheme 2. The proposed mechanistic route for synthesis of (2*E*)-substituted styryl-4-bromophenyl ketones by potassium hydrogen phthalate assisted aldol condensation.

Table 2. The solvent influence on the yields of synthesized (2*E*)-substituted styryl-4-bromophenyl ketones

Entry	X	EtOH	MeOH	MeCN	DO	DCM	*i*-PrOH	THF
1a	H	87	79	38	57	61	58	72
1b	3-Cl	89	87	40	50	62	56	69
1c	4-Cl	88	85	42	52	63	55	68

Entry	X	EtOH	MeOH	MeCN	DO	DCM	*i*-PrOH	THF
1d	4-F	85	83	35	55	59	60	70
1e	3-OH	83	80	33	53	62	61	71
1f	3-OCH_3	90	88	46	58	68	65	75
1g	4-CH_3	89	86	41	54	66	63	73
1h	3-NO_2	80	76	36	49	57	56	65
1i	4-NO_2	82	79	32	50	58	57	64

EtOH: ethanol; MeOH: methanol; MeCN: acetonitrile; DO: dioxane; DCM: dichloromethane; *i*-PrOH: isopropanol; THF: tetrahydrofuran

The vibrational conformers *s-cis* and *s-trans* of synthesized enones are showed in Figure 1.

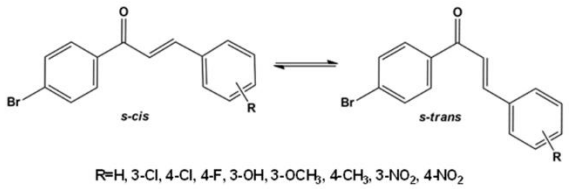

Figure 1. The *s-cis* and *s-trans* conformers of (2*E*)-substituted styryl-4-bromophenyl ketones

The spectroscopical data of enone 1a and unreported enones **1e** and **1f** are summarized as follows.

(***E*)-1-(4-Bromophenyl)-3-phenyl prop-2-ene-1-one (1a):** FT-IR (KBr, cm^{-1}) ν = 1657 ($CO_{s\text{-}cis}$), 1603 ($CO_{s\text{-}trans}$), 692 (C=C_{op}); ^{1}H NMR δ = 7.627 (d, 1H, H_α), 7.933 (d, 1H, H_β), 7.46-8.11 (9H, m, 9H, Ar-H); ^{13}C NMR δ=122.30 (C_α), 145.03 (C_β), 188 (CO), 127.81-137.00 (Ar-C). Mass (m/z) = 287 [M^+], 289 [M^{2+}].

(***E*)-1-(4-Bromophenyl)-3-(3-hydroxyphenyl) prop-2-en-1-one (1e):** FT-IR (KBr, cm^{-1}) ν = 1682 ($CO_{s\text{-}cis}$), 1653 ($CO_{s\text{-}trans}$), 975 (C=C_{OP}); ^{1}H NMR δ = 7.747 (d, 1H, H_α), 7.423 (d, 1H, H_β), 6.965 (d, 1H, OH), 7.145-7.872 (m, 8H, Ar-H); ^{13}C NMR δ = 121.67 (C_α), 145.50 (C_β), 189 (CO), 128.09-136.79 (Ar-C). Anal. for M.F.: $C_{15}H_{11}BrO_2$, Found (Calcd.): C 59.46 (59.40), H 3.67 (3.60) %. Mass (m/z) = 303 [M^+], 305 [M^{2+}], 285, 224, 209, 183, 155, 148, 120, 94, 79, 18.

(***E*)-1-(4-Bromophenyl)-3-(3-methoxyphenyl) prop-2-en-1-one (1f):** FT-IR (KBr, cm^{-1}) ν = 1662 ($CO_{S\text{-}cis}$), 1601($CO_{S\text{-}trans}$), 982 (C=C_{OP}); ^{1}H NMR δ = 7.772 (d, 1H, H_α), 7.445 (d, 1H, H_β), 3.654 (s, 3H, -OCH_3), 7.004-7.891 (m, 8H, Ar-H); ^{13}C NMR δ = 121.17 (C_α), 145.3 (C_β),189 (CO), 55.39 (-OCH_3), 128.91-138.67 (Ar-C). Anal. for M.F.: $C_{16}H_{13}BrO_2$, Found (Calcd.): C 60.54 (60.56), H 3.99 (4.10) %. Mass (m/z) = 317 [M^+], 285, 238, 209, 183, 162, 155, 134, 108, 79,32.

These data are well supported for the synthesis confirmation of the (2*E*)-substituted styryl-4-bromophenyl enones.

3.2 Frontier molecular orbitals analysis

Frontier molecular orbitals, comprising the HOMO and LUMO, play key roles in chemical reactivity, where the HOMO donates electrons and the LUMO accepts them. The chemical characteristics, biological effects, and intermolecular charge transfer (ICT) mechanisms of a molecule are all significantly influenced by these orbitals. The electronic properties of molecules, including their reactivity, kinetic stability, and ability to conduct electrons, are strongly influenced by the energy levels of the HOMO and LUMO, as well as the magnitude of the HOMO–LUMO gap [23]. The large HOMO-LUMO energy difference indicates lesser polarizability, lower chemical reactivity, increased kinetic stability, and higher molecular hardness. On the other hand, a narrower energy gap indicates greater polarizability, increased chemical reactivity, lesser kinetic stability, and higher molecular softness [24, 25]. These quantum chemical indices have multiple uses as well as correlate with several chemical and biochemical characteristics [26, 27]. Using DFT-B3LYP/6-311G(d,p) calculations, we performed FMO analysis to derive global electronic and reactivity descriptors for the synthesized chalcone analogues **(1a–i),** a method well-regarded for probing molecular properties and biological relevance. The HOMO, LUMO picture and energy gap (ΔE) values are presented in Table 2. The energies of the highest occupied molecular orbital (HOMO) of synthesized compounds **(1a-i)** range from -6.481 to -7.349 eV, which shows all have almost similar values. The synthesized compounds exhibit LUMO energies in the range of –2.571 to –3.646 eV. The energy gaps (ΔE) of the synthesized compounds derived from frontier molecular orbitals range between 3.703 eV and 4.152 eV. All the compounds have almost similar energy gaps. Out of these compounds, **1i** has the lowest energy gap value, and compound **1b** has the highest energy gap value, which indicates that compound **1**i has more reactivity and polarizability but is less stable, and compound **1b** has moderate reactivity and is more stable. The ascending order of energy gaps for synthesized compounds is as follows: **1i < 1h < 1f < 1g < 1e < 1c < 1d < 1a < 1b.** The energy gap values are presented in Figure 2.

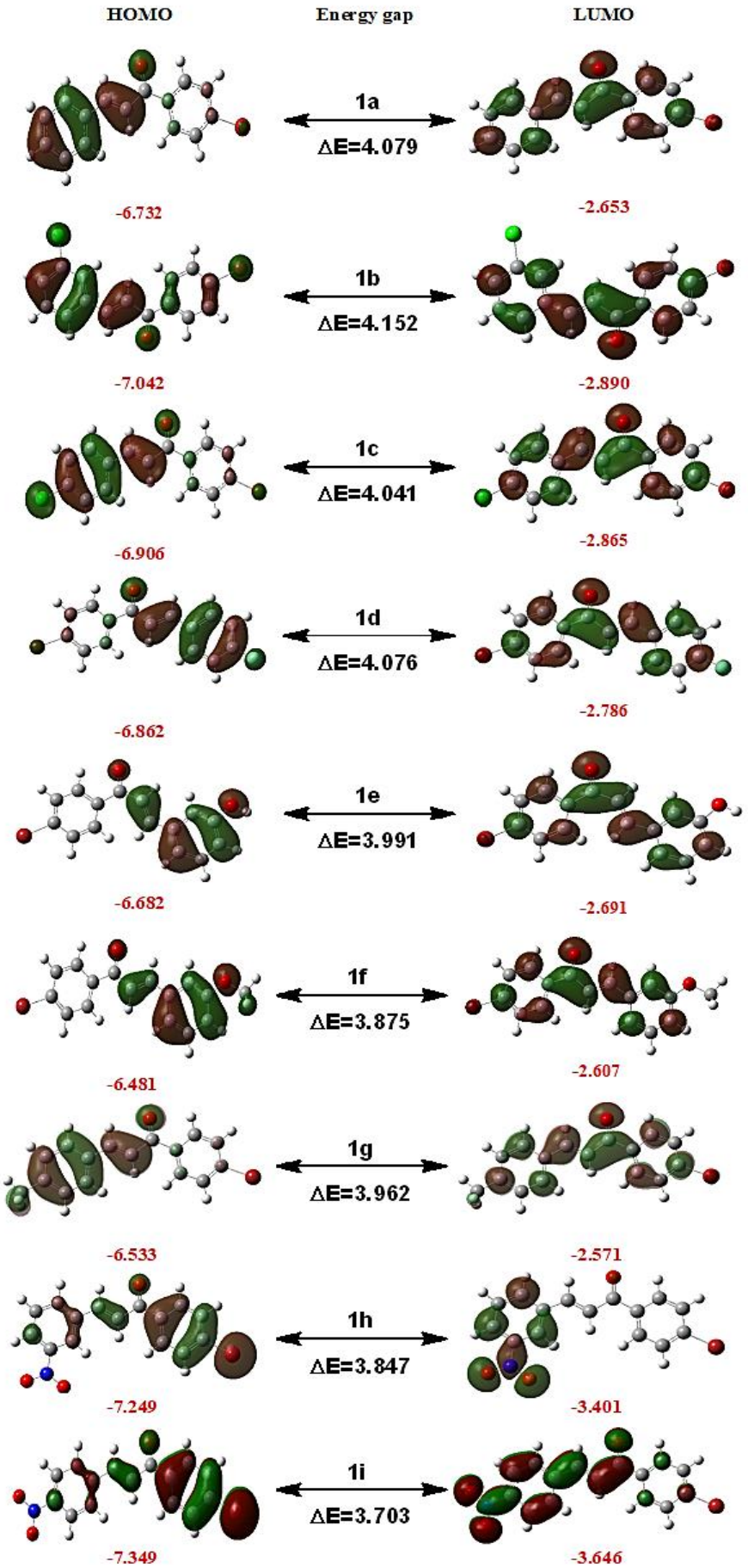

Figure 2. Frontier molecular orbitals of (2*E*)-substituted styryl-4-bromophenyl ketones (**1a-i**)

3.2. Global reactivity analysis of 4-bromophenyl chalcone derivatives (1a-i)

The FMO method was used to calculate a number of reactivity measurements, such as electron affinity (EA), ionization energy (IP), electronegativity (χ), softness (σ), and hardness (η). E_{HOMO} is connected to ionization energy, which gives details about how an electron is removed from a molecule [26]. Computational properties of 4-bromophenyl chalcone derivatives **(1a-i)** have been given in Table 3. The ionization energies of the synthesized compounds were obtained in the range between 6.481 and 7.349 eV. Compound **1i** has a maximum ionization energy of 7.349 eV. Compound **1f** has the lowest ionization energy of 6.481 eV, which indicates the lower ionization energy and the simplest to remove an electron. Chemical reactivity is largely dependent on electron affinity (EA). EA is defined as the energy released upon the addition of an electron to a molecule. It is the opposite of the IP. The electron affinity values of synthesized compounds are obtained in the range from 2.571 to 3.646 eV. Compound **1g** has the lowest EA value of 2.571 eV, and compound **1i** has the highest EA value of 3.646 eV.

The polarizability of a molecule can also be evaluated by its softness and hardness. A molecule with a greater softness value and a lower hardness value is more polarizable. From this FMO orbital analysis, compound **1i** has a lower hardness and a high softness value. Hence, the compound **1i** has higher polarizability and chemical reactivity.

Table 3. Computational properties of (2*E*)-substituted styryl-4-bromophenyl ketones (**1a-i**)

Entry	IP	EA	ΔE	η	σ	μ	χ	Ω
1a	6.732	2.653	4.079	2.039	0.490	4.677	-4.692	5.398
1b	7.042	2.890	4.152	2.076	0.481	4.966	-4.966	5.939
1c	6.906	2.865	4.041	2.020	0.495	4.886	-4.886	5.907
1d	6.862	2.786	4.076	2.038	0.490	4.824	-4.824	5.710
1e	6.682	2.691	3.991	1.995	0.501	4.687	-4.687	5.503
1f	6.481	2.607	3.875	1.937	0.516	4.544	-4.544	5.329
1g	6.533	2.571	3.962	1.981	0.504	4.552	-4.552	5.231
1h	7.249	3.401	3.847	1.924	0.519	5.325	-5.325	7.370
1i	7.349	3.646	3.703	1.852	0.539	5.498	-5.498	8.162

IP - ionization potentials; EA- electron affinity; ΔE - energy gap; η - hardness; σ- softness, μ - chemical potentials; χ – electronegativity; ω – electrophilicity.

3.3. Molecular electrostatic potential

By using color grading, MEP mapping provides insights into molecular geometry and highlights regions of positive, negative, and neutral electrostatic potential. In the MEP map, red regions represent areas of high electron density, making them favorable sites for electrophilic attack, whereas blue regions indicate electron-deficient zones, which are suitable for nucleophilic attack [28]. The MEP surfaces of the synthesized compounds (**1a-i**) are given in Figure 3. All the synthesized compounds show a red color in the oxygen zone, which indicates an electrophilic zone. However, the blue color zone of the MEP of the compounds (**1a-i**) is other than the oxygen zone; hence, the blue zone is a favorable nucleophilic region.

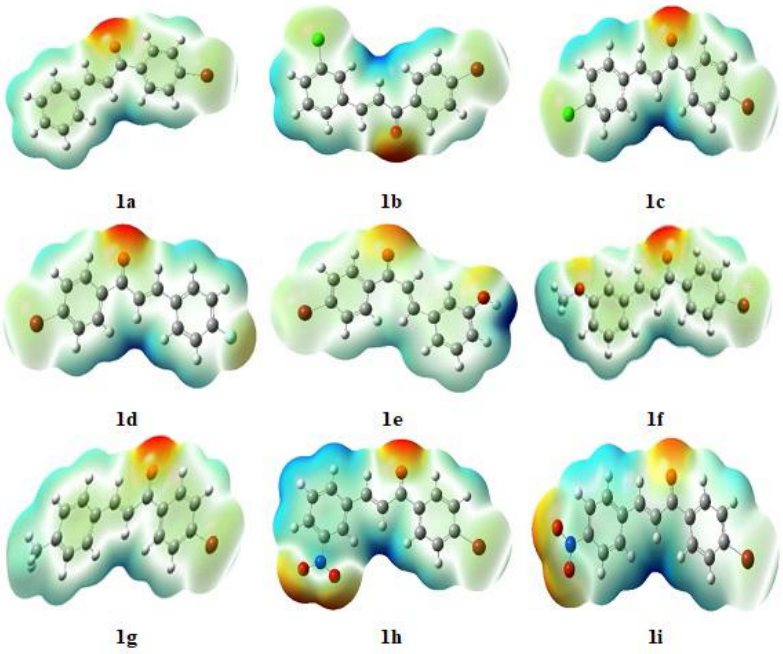

Figure 3. MEP surface of (2*E*)-substituted styryl-4-bromophenyl ketones (**1a - i**).

3.4. Molecular docking studies 4-bromophenyl chalcone derivatives (1a-i)

In the present discussion, the synthesized compounds were docked against D-glutamate ligase (PDB ID: 1UAG) bacterial protein. The docking results are shown in the Table 4. This table contains 3D poses of the compound, binding energy, and binding interaction between the amino acids and the synthesized compounds.

Table 4. Molecular docking results of (2*E*)-substituted styryl-4-bromophenyl ketones

Entry	3D pose	Binding energy	H-bond interaction	Other interactions	Interaction types
1a	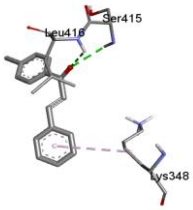	-6.45	SER A:415 LEU A:416	LYS.A:348	Pi alkyl
1b	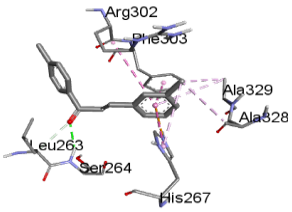	-6.29	SER: A .264	ALA.A:329 HIS.A:267 PHE.A:303 ARG.A:302 ALA.A:302	C-H-Bond Pi-Cation Pi-Pi-Stacked Amide-Pi stacked Alkyl
1c	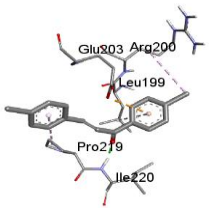	-6.63	ILE:220	GLU.A:203 ARGA.A:200 PRO.A:219	Pi-Anion Alkyl Pi-Alkyl
1d	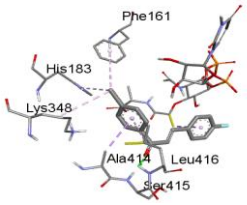	-5.55	LEU.A:416 SER.A:415	ALA.A:414 HIS.A:183 LYS.A:348 PHE.A:161 ALA.A:414	Pi-Sigma Alkyl Alkyl Alkyl Pi-Alkyl
1e	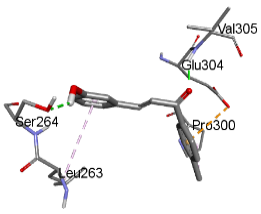	-6.25	VAL A:305 SER.A:264	GLU.A:304 PRO.A:300 LEU.A:263	Pi-Anion Alkyl Pi-Alkyl
1f	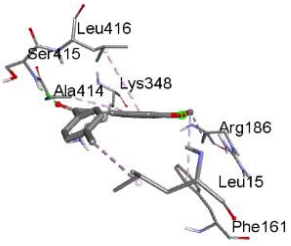	-6.29	SER.A:415	LEU.A:15 PHE.A:161 ARGA.A:186 ALA.A:415 LEU.A:416 LYS.A:348	Alkyl Alkyl Alkyl Pi-alkyl Pi-alkyl Pi-alkyl

Entry	3D pose	Binding energy	H-bond interaction	Other interactions	Interaction types
1g	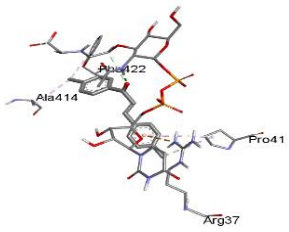	-6.56	-	PHE.A:422 ARG.A:37 ALA.A:414 PRO.A:41	C-H bond Pi-Carbon Alkyl Pi-alkyl
1h	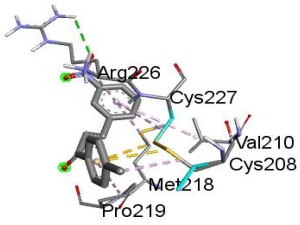	-5.79	ARGA:226	CYS.A:227 CYS.A:208 VAL.A:210 MET. A:218 PRO.A:219	Pi-Donor H-bond Pi-sulphur Alkyl Alkyl Pi-alkyl
1i	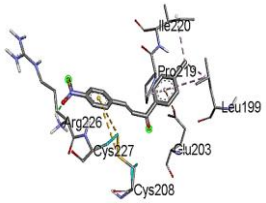	-6.5	ARG.A:226	GLU A:203 CYS.A:227 CYS.A:208 PRO. A:219 ILE.A:220 LEU.A:199	Pi-anion Pi-sulphur Pi-sulphur Pi-alkyl Alkyl Alkyl

The binding energy of the synthesized compounds **(1a-i)** ranges from -5.55 to -6.63 kcal/mol. The **1c** compound shows the highest binding affinity with target protein 1UAG. The compound **1c** has one hydrogen bond interaction with ILE: 220 and hydrophobic interactions with the GLU 203, ARG 200, and PRO 219 amino acid residues. Compound **1g** does not have hydrogen bond interaction, but it has only hydrophobic interactions with PHE 422, ARG 37, ALA 414, PRO 41. Hence, compound **1g** has moderate antibacterial activity. The docking results reveal that all synthesized compounds have good antibacterial activity except **1h**, because these compounds (**1a, 1b, 1c, 1d, 1e, 1f, 1h**, and **1i**) have a good binding insight with the 1UAG protein.

3.5. ADMET analysis

The graphical representation for the drug-like properties of synthesized (2*E*)-substituted styryl-4-bromophenyl ketones (**1a-i**) is shown in Figure 4.

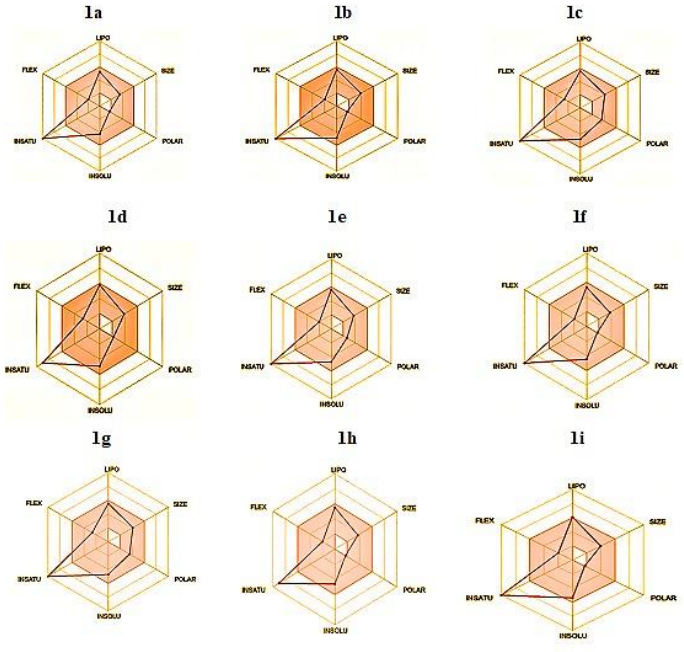

Figure 4. ADME radar absorption structure (2*E*)-substituted styryl-4-bromo ketones

The bioavailability radar structure provides quick understanding of the data, which is useful to understand the drug-likeness property of compounds (**1a-i**). The colored zone indicates the distinguished physicochemical properties for oral bioavailability. POLAR (polarity): 20 $Å^2$ < TPSA < 130 $Å^2$; INSOLU (insolubility): -6 < log S < 0; INSATU (unsaturation): 0.25 < fraction Csp^3 < 1; LIPO (lipophilicity): -0.7 < log P3 < + 5.0; FLEX (flexibility): 0 < number of rotatable bonds < 9; SIZE: 150 g/mol < molecular weight < 500 g/mol [18]. Table 5 shows the physicochemical properties of the chalcone series (**1a-i**). Based on Lipinski's and Veber's rules, the synthesized compounds **1a, 1c, 1d, 1e**, and **1g** show zero violations, except **1c**, **1d**, and **1g**. The molecular weight of the compounds (**1a-i**) range from 287.15 g/mol to 332.15 g/mol. This shows that all the compound have a range of molecular weight below 500. The hydrogen bond acceptor range is 3 to 1 (≤ 10) and the number of hydrogen bond donor atoms was zero (≤ 5) for all synthesized compounds. This indicates that all the synthesized compounds have optimal physicochemical properties based on Lipinski's rule of 5.

Table 5. Physico-chemical properties of (2*E*)-substituted styryl-4-bromophenyl ketones

Entry	Lipinski's violations (≤1)	Based on Lipinski 's Rule				Veber's rule		
		MW (≤500)	HBA (≤10)	HBD (≤5)	MLOGP	NROTB (≤10)	TPSA (130 Å)	ABS%
1a	0	287.15	1	0	4.08	3	17.07	103.11
1b	1	321.6	1	0	4.59	3	78.96	81.75
1c	1	321.60	1	0	4.59	3	17.07	103.11
1d	1	305.14	2	0	4.47	3	17.07	103.11
1e	0	303.15	1	1	3.42	3	37.30	103.12
1f	0	317.18	2	0	3.66	4	26.30	99.92
1g	1	301.18	1	0	4.32	3	17.07	103.11
1h	0	287.70	3	0	2.70	4	62.89	87.30
1i	0	332.15	3	0	2.82	4	62.89	87.30

Lipophilicity has a major role in determining a number of ADME features. Drug molecule's distribution between the lipid composition of the cell membrane and the aqueous environment outside of it; this is quantified by the log P. Compounds with a lower log P value are therefore more polar and have less permeability across their lipid bilayers. Compounds exhibiting higher log P values tend to be less polar and exhibit lower water solubility. They have great lipophilicity, corresponding to the predicted log P values, which range from 2.70 to 4.59. The absorption percentage of the synthesized compound (**1a-i**) ranges from 81.75 to 103.11. The synthesized compounds (**1a–i**) demonstrated strong pharmacokinetic properties, including high gastrointestinal absorption and blood–brain barrier permeability (Table 6), which reflects their potential for rapid digestion and effective absorption in the small intestine.

Table 6. Pharmacokinetic properties of (2*E*)-substituted styryl-4-bromophenyl ketones

Entry	GI	BBB	P-gp	CYP1A2	CYP2C19	CYP2C9	CYP2D6	CYP3	Bioavailability score
1a	High	Yes	No	Yes	Yes	Yes	No	No	0.55
1b	High	Yes	No	Yes	Yes	Yes	No	No	0.55
1c	High	Yes	No	Yes	Yes	Yes	No	No	0.55
1d	High	Yes	No	Yes	Yes	Yes	Yes	No	0.55
1e	High	Yes	No	Yes	Yes	Yes	No	No	0.55
1f	High	Yes	No	Yes	Yes	Yes	Yes	No	0.55
1g	High	Yes	No	Yes	Yes	Yes	Yes	No	0.55
1h	High	Yes	No	Yes	Yes	Yes	Yes	No	0.55
1i	High	Yes	No	Yes	Yes	Yes	No	No	0.55

A variety of cytochromes (CYPs) control drug metabolism, with CYP1A2, CYP2C19, CYP2C9, CYP2D6, and CYP3A4 specifically controlling the biotransformation of drug compounds. All the compounds (**1a-i**) have good **CYP1A2, CYP2C19**, and **CYP2C9** inhibition. These findings evaluate the compounds, which showed diverse effects, exhibiting their capacity to inhibit certain kinds of enzymes. This data is crucial for understanding the pharmacokinetic effects of co-administration and for evaluating any interactions with other medications that are processed by these enzymes. The toxicity prediction results are shown in Table 7. The toxicity prediction of the synthesized compounds (**1a-i**) revealed that the toxicity class classification and LD_{50} value represent all the compounds are non-toxic, except **1e**. Hence, the **1e** compound has a 1048 mg/kg LD_{50} value and a class 4 toxicity classification, which shows as harmful when it is swallowed. The toxicological prediction results show the endpoints of hepatotoxicity, carcinogenicity, mutagenicity, and cytotoxicity. The compounds **1a, 1b, 1c, 1d**, and **1h** are all inactive (negative) in hepatotoxicity. All the synthesized compounds are inactive in cytotoxicity, except **1d** and **1e**. The mutagenicity prediction result shows that all the compounds are inactive, except **1i** and **1h**. All the compounds have shown carcinogenicity, except **1e**. ADMET prediction results indicate that all synthesized

compounds could be viable therapeutic candidates, leading to further investigation.

Table 7. Toxicity prediction results of (2*E*)-substituted styryl-4-bromophenyl ketones

Entry	LD_{50} (mg/kg)	Toxicity class	Organ toxicity			
			Hepatotoxicity	Cytotoxicity	Mutagenicity	Carcinogenicity
1a	3000	5	Negative	Negative	Negative	Positive
1b	3000	5	Negative	Negative	Negative	Positive
1c	3000	5	Negative	Negative	Negative	Positive
1d	3000	5	Negative	Positive	Negative	Positive
1e	1048	4	Positive	Positive	Negative	Negative
1f	2100	5	Positive	Negative	Negative	Positive
1h	3000	5	Negative	Negative	Negative	Positive
1g	3000	5	Positive	Negative	Positive	Positive
1i	3000	5	Positive	Negative	Positive	Positive

3.6. Secondary enzyme target prediction

In the present investigation, we used the "Swiss Target Prediction" bioinformatics software to make *in silico* enzyme target predictions for the synthesized compounds utilizing a ligand-based technique. Since bioactive compounds interact with protein receptors or other macromolecular sites to exert their action, *in silico* screening provides a fast and efficient approach for identifying drug-interacting sites and potential therapeutic targets in biomolecules [29]. As a result, scientists are creating novel drug candidates with specialized functions, possibly focusing on certain biochemical pathways that have rarely been investigated. Finding secondary targets has two benefits in the field of research and creation of bioactive compounds. First of all, it helps to identify possible negative side effects, which reduces the potential of toxicity-related clinical trial failures. Secondly, by identifying new targets, this method can uncover novel applications for current medications. Taking these factors into account, we used the "Swiss Target Prediction" bioinformatics software [30] to determine the most likely enzyme target for the synthesized compounds (**1a-i**) using ligand-based target prediction. The expected outcomes for our synthetic compounds are shown in the Figure 5.

In silico, ligand-based target prediction indicates that molecules such as **1a, 1d**, and **1e** have 26.7%; **1b, 1c, 1f**, and **1i** have 13.3%, and **1h** has 20.0% of oxidoreductase inhibition. Hence, these compounds may act as a potential oxidoreductase inhibitor. Compounds **1a** and **1d** have 20.0%, **1e, 1g**, and **1h** have 13.3%, and **1f** and **1i** had 6.7% good enzyme inhibition. Therefore, these compounds may act as a good enzyme inhibitor. Furthermore, compounds **1a, 1c, 1f**, and **1h** have 13.3% inhibition, **1e** and **1i** have 6.7% inhibition. Enones **1b** had 26.6%, and **1g** had 20.0% and could function as a Family A GPCR ligand inhibitor. Enones **1b**, **1d**, and **1e** have shown 6.7% inhibition and function as kinase inhibitors. Compounds **1b, 1e**, and **1h** have 6.7% inhibition. Enones **1c** and **1g** have 13.3% inhibition and they functioned as protease enzyme inhibitors. Compound **1f** shows 20% inhibition. Remaining enones **1a**, **1b**, **1c**, **1e**, **1h**, and **1i** have 6.7% inhibition and they functioned as a ligand-gated ion channel inhibitors. The secondary enzyme target prediction study reveals that the synthesized compounds may have potential enzyme inhibition targets for further development of drugs.

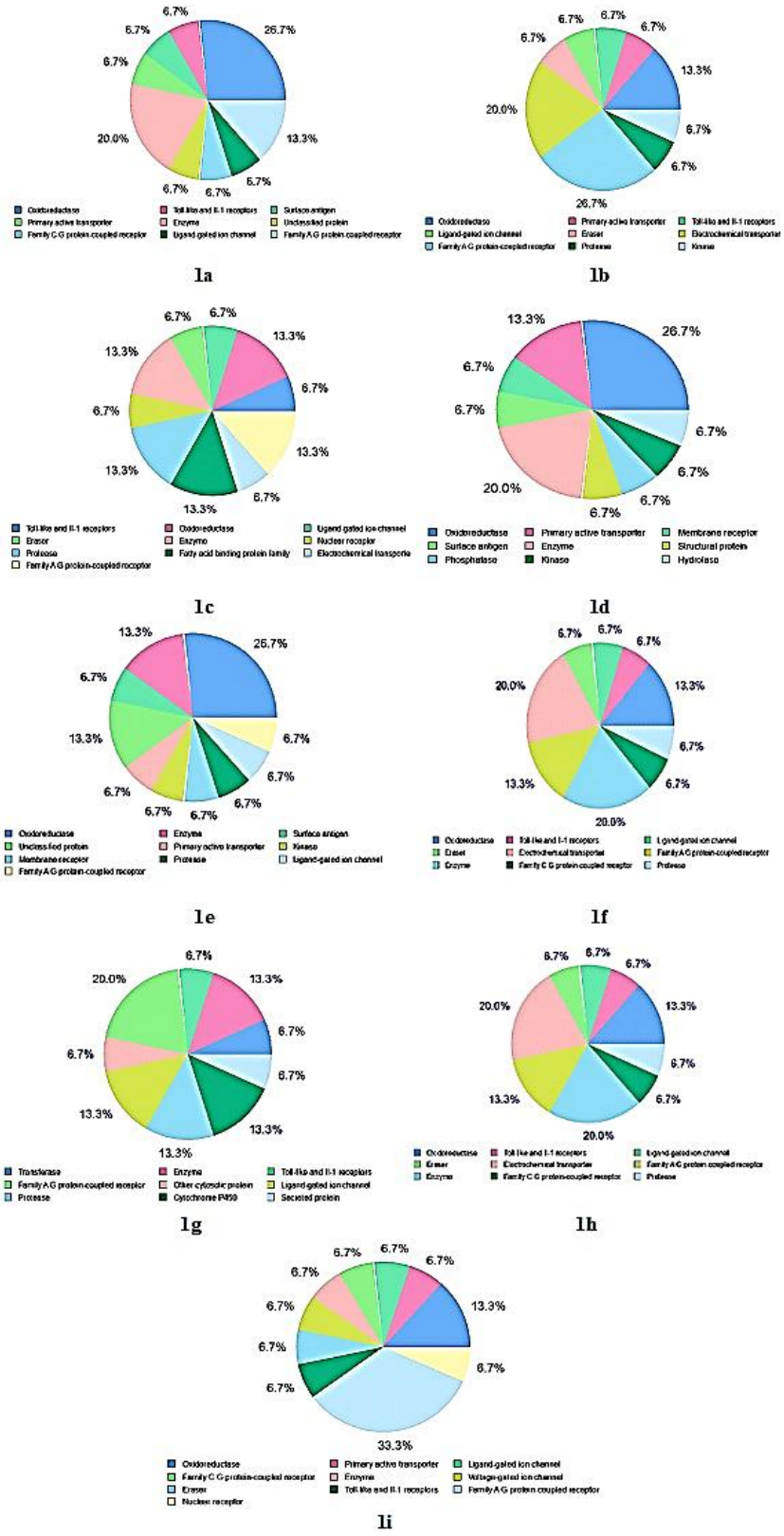

Figure 5. The outcomes of secondary enzyme target prediction with (2*E*)-substituted styryl-4-bromophenyl ketones

4. Conclusions

In summary, the obtained chalcone analogues (**1a-i**) show remarkable promise in a number of fields, and their effective synthesis provides a strong basis for future advancements in medicinal chemistry**.** The synthesized 4-bromophenyl chalcone derivatives are examined with various computational studies like DFT analysis, molecular docking, ADMET analysis and secondary enzyme target prediction. Out of these, the Density Functional Theory (DFT) analysis reveals that the compound **1i** has most potential chemical reactivity

due to polarizability. Hence, the compound **1i** exhibits an energy gap between the HOMO and LUMO of 3.703 eV, which is the lowest energy gap value and a higher softness value compared with other chalcones. From the molecular docking results, compound **1c** has the highest binding affinity with D-glutamate ligase 1UAG bacterial protein. Based on the ADMET prediction result, it supports that all the synthesized compounds may be potential drug candidates for future pharmacological development. Finally, the secondary enzyme target prediction concludes most of the synthesized compounds act as a good enzyme inhibitor of oxidoreductase, protease, and kinase enzymes. Chalcone analogues (**1a-i**) offer promising research opportunities for therapeutic applications in chemistry and biology.

Conflict of interest

The authors declare that there is no conflict of interest regarding this research article.

Supplementary information

NMR spectra of compounds **1a**, **1e**, and **1f** and the mass spectra and its fragments of compounds **1e** and **1f** are provided in the supplementary information file.

References

[1]. M. I. Abdullah, A. Mahmood, M. Madni, S. Masood, M. Kashif, Synthesis, characterization, theoretical, anti-bacterial and molecular docking studies of quinoline based chalcones as a DNA gyrase inhibitor, Bioorganic Chemistry 54 (2014) 31–37. DOI: 10.1016/j.bioorg.2014.03.006

[2]. M.S. Alam, S.M.M. Rahman, D.U. Lee, Synthesis, biological evaluation, quantitative-SAR and docking studies of novel chalcone derivatives as antibacterial and antioxidant agents, Chemical Papers 69 (2015) 1118-1129. DOI: 10.1515/chempap-2015-0113

[3]. P. Gayathri, I. Muthuvel, P. Mayavel, K. Ranganathan, V. Usha, V. Mala, G. Thirunarayanan, Microwave assisted synthesis and evaluation of antimalarial potencies of some 8-quinoline enones, Ovidius University Annals of Chemistry 36 (2025) 66-72. DOI: 10.2478/auoc-2025-0008

[4]. G. Wang, J. Qiu, X. Xiao, A. Cao, F. Zhou, Synthesis, biological evaluation and molecular docking studies of a new series of chalcones containing naphthalene moiety as anticancer agents, Bioorganic Chemistry 76 (2018) 249–257. DOI: 10.1016/j.bioorg.2017.11.017

[5]. P. Gayathri, J. Divya, I. Muthuvel, V. Usha, M. Retna, G. Thirunarayanan, A greener synthesis, molecular docking, antimicrobial and antimalarial activities of some unsaturated ketones, Indian Journal of Chemistry 64 (2025) 670-681. DOI: 10.56042/ijc.v64i7.12246

[6]. C. Díaz-Tielas, E. Graña, M.J. Reigosa, A.M. Sánchez-Moreiras, Biological activities and novel applications of chalcones, Planta Daninha 34 (2016) 607–616. DOI: 10.1590/s0100-83582016340300022

[7]. G.S.B. Viana, M.A.M. Bandeira, F.J.A. Matos, Analgesic and anti-inflammatory effects of chalcones isolated from *Myracrodruon urundeuva* Allemão, Phytomedicine 10 (2003) 189–195. DOI: 10.1078/094471103321659924

[8]. J.C. Trivedi, J.B. Bariwal, K.D. Upadhyay, Y.T. Naliapara, S.K. Joshi, C.C. Pannecouque, E. de Clercq, A.K. Shah, Improved and rapid synthesis of new coumarinyl chalcone derivatives and their antiviral activity, Tetrahedron Letters 48 (2007) 8472–8474. DOI: 10.1016/j.tetlet.2007.09.175

[9]. R.A. Gupta, S.G. Kaskhedikar, Synthesis, antitubercular activity, and QSAR analysis of substituted nitroaryl analogs: chalcone, pyrazole, isoxazole, and pyrimidines, Medicinal Chemistry Research 22 (2013) 3863–3880. DOI: 10.1007/s00044-012-0385-3

[10]. R. Arulkumaran, S. Vijayakumar, S.P. Sakthinathan, D. Kamalakkannan, K. Ranganathan, R. Suresh, R. Sundararajan, G. Vanangamudi, G. Thirunarayanan, Preheated fly-ash catalyzed aldol condensation: efficient synthesis of chalcones and antimicrobial activities of some 3-thienyl chalcones, Journal of the Chilean Chemical Society 58 (2013) 1684–1690. DOI: 10.4067/S0717-97072013000200008

[11]. K. Ranganathan, R. Suresh, D. Kamalakkannan, R. Arulkumaran, R. Sundararajan, S.P. Sakthinathan, S. Vijayakumar, G. Vanangamudi, K. Thirumurthy, P. Mayavel, G. Thirunarayanan, Electrochemical reduction potential correlation of some insect antifeedant potent 2-phenothiazinyl chalcones, International Letters of Chemistry Physics and Astronomy 4 (2012) 66–75.

[12]. S. Nasir Abbas Bukhari, M. Jasamai, I. Jantan, W. Ahmad, Review of methods and various catalysts used for chalcone synthesis, Mini-Reviews in Organic Chemistry 10 (2013) 73–83. DOI: 10.2174/1570193X11310010006

[13]. S. Burmaoglu, E.A. Kazancioglu, R. Kaya, M. Kazancioglu, M. Karaman, O. Algul, I. Gulcin, Synthesis of novel organohalogen chalcone derivatives and screening of their molecular docking study and some enzymes inhibition effects, Journal of Molecular Structure 1208 (2020) 127868. DOI: 10.1016/j.molstruc.2020. 127868

[14]. S. Vijayakumar, G. Vanangamudi, G. Thirunarayanan, Synthesis, effect of substituents and antimicrobial activities of some 4-bromophenyl chalcones, World Scientific News 54 (2018) 132-152.

[15]. K.B. Gangurde, V.A. Adole, D.S. Ghotekar, Computational study: Synthesis, spectroscopic (UV–vis, IR, NMR), antibacterial, antifungal, antioxidant, molecular docking and ADME of new (E)-5-(1-(2-(4-(2,4-dichlorophenyl)thiazol-2-yl)hydrazineylidene)ethyl)-2,4-dimethylthiazole, Results in Chemistry 6 (2023) 101093. DOI: 10.1016/j.rechem.2023.101093

[16]. A. Weyesa, R. Eswaramoorthy, Y. Melaku, E. Mulugeta, Antibacterial, docking, DFT and ADMET properties evaluation of chalcone-sulfonamide derivatives prepared using ZnO nanoparticle catalysis, Advances and Applications Bioinformatics and Chemistry 14 (2021) 133–144. DOI: 10.2147/AABC.S336450

[17]. R. Ahsan, S. Paul, M.S. Alam, A.F.M. M. Rahman, Synthesis, biological properties, *in silico* ADME, molecular docking studies, and FMO analysis of chalcone derivatives as promising antioxidant and antimicrobial agents, ACS Omega 10 (2025) 4367–4387. DOI: 10.1021/acsomega.4c06897

[18]. F. Akhter, S.S. Marufa, S.M.A.U. Shohag, H. Nishino, M.S. Alam, Md.A. Haque, M.M. Rahman, Synthesis, antimicrobial evaluation, ADMET prediction, molecular docking and dynamics studies of pyridine and thiophene moiety-containing chalcones, Royal Society Open Science 12 (2025) 241411. DOI: 10.1098/ rsos.241411

[19]. T. Nawaz, A. Tajammal, A.W. Qurashi, M. Nisa, D.N. Binjawhar, M. Iqbal, Synthesis, antibacterial, antibiofilm, and docking studies of chalcones against multidrug resistance pathogens, Heliyon 10 (2024) e30618. DOI: 10.1016/j.heliyon. 2024.e30618

[20]. R.Z. Batran, E.Y. Ahmed, H.M. Awad, N.A. Abdel Latif, Naturally based pyrazoline derivatives as aminopeptidase N, VEGFR2 and MMP9 inhibitors: design, synthesis and molecular modeling, RSC Advances 14 (2024) 22434–22448. DOI: 10.1039/D4RA01801J

[21]. M.H. Shaikh, D.D. Subhedar, L. Nawale, D. Sarkar, F.A. Kalam Khan, J.N. Sangshetti, B.B. Shingate, 1,2,3-Triazole derivatives as antitubercular agents: synthesis, biological evaluation and molecular docking study, Medicinal Chemistry Communications 6 (2015) 1104–1116. DOI: 10.1039/C5MD00057B

[22]. D. Gfeller, A. Grosdidier, M. Wirth, A. Daina, O. Michielin, V. Zoete, SwissTargetPrediction: a web server for target prediction of bioactive small molecules, Nucleic Acids Research 42 (2014) W32–W38. DOI: 10.1093/nar/gku293

[23]. V. Hadigheh Rezvan, Molecular structure, HOMO–LUMO, and NLO studies of some quinoxaline 1,4-dioxide derivatives: Computational (HF and DFT) analysis, Results in Chemistry 7 (2024) 101437. DOI: 10.1016/j.rechem.2024.101437

[24]. X. Zhang, R. Jin, Rational design of low-band gap star-shaped molecules with 2,4,6-triphenyl-1,3,5-triazine as core and diketopyrrolopyrrole derivatives as arms for organic solar cells applications, Frontiers in Chemistry 7 (2019) 122. DOI: 10.3389/fchem.2019.00122

[25]. S.A. Halim, H. Hamad, T.E. Ali, Deeper insights into the density functional theory of structural, optical, and photoelectrical properties using 5-[(4-oxo-4H-chromen-3-yl) methylidene]-4-oxo (thioxo)-6-thioxo-2-sulfido-1, 3, 2-diazaphosphinanes, Optical and Quantum Electronics 55 (2023) 458. DOI:10.1007/s11082-023-04661-8

[26]. N. Dinesh Kumar, S. Rajmohan, K. Selvakumar, D. Rajamanickam, G. Thirunarayanan, M. Swaminathan, Eco-friendly sustainable synthesis of 2-phenoxy Schiff bases supported on SO_4^{2-}−TiO_2: a comprehensive study of structure and antimicrobial activity, Journal of Molecular Structure 1343 (2025) 142824. DOI: 10.1016/j.molstruc.2025.142824

[27]. P. Gayathri, K.R. Anam, J. Divya, S. Balasundari, P. Sudha, P. Mayavel, I. Muthuvel, V. Usha, V. Sathiyendiran, B. Krishnakumar, K. Ranganathan, N. Dinesh Kumar, S. Rajasri¸ G. Thirunarayanan, Synthesis, spectroscopical studies, DFT, ADMET, molecular docking analysis, antimalarial, antimicrobial activities of some *E*-imines and XRD structure of (*E*)-*N*-(2-bromobenzylidene)-2-(trifluoromethyl)benzenamine, Indian Journal of Chemistry 64 (2025) 1097-1111. DOI: 10.56042/ijc.v64i11.24230

[28]. H.M. Al-Maqtari, A.H. Hasan, M. Suleiman, M.A. Ahmad Zahidi, M.A. Noamaan, P. Alexyuk, M. Alexyuk, A. Bogoyavlenskiy, J. Jamalis, Benzyloxychalcone hybrids as prospective acetylcholinesterase inhibitors against Alzheimer's disease: Rational design, synthesis, *in silico* ADMET prediction, QSAR, molecular docking, DFT, and molecular dynamic simulation studies, ACS Omega (2024) 32901-32919. DOI: 10.1021/acsomega. 4c03679

[29]. E. Lounkine, M.J. Keiser, S. Whitebread, D. Mikhailov, J. Hamon, J.L. Jenkins, P. Lavan, E. Weber, A.K. Doak, S. Côté, B.K. Shoichet, L. Urban, Large-scale prediction and testing of drug activity on side-effect targets, Nature 486 (2012) 361–367. DOI: 10.1038/nature11159

[30]. A. Daina, O. Michielin, V. Zoete, SwissTargetPrediction: updated data and new features for efficient prediction of protein targets of small molecules, Nucleic Acids Research 47 (2019) W357–W364. DOI: 10.1093/nar/gkz382

Received: 15.09.2025
Received in revised form: 20.12.2025
Accepted: 21.12.2025